Agricultural Water Management 258 (2021) 107181

Contents lists available at ScienceDirect

Agricultural Water Management

journal homepage: www.elsevier.com/locate/agwat

Comparisons among four different upscaling strategies for cultivar genetic parameters in rainfed spring wheat phenology simulations with the DSSAT-CERES-Wheat model

Shang Chen [a,b,c], Liang He [d], Yinxuan Cao [a,c], Runhong Wang [a,c], Lianhai Wu [e], Zhao Wang [f], Yufeng Zou [a,c], Kadambot H.M. Siddique [g], Wei Xiong [h], Manshuang Liu [i], Hao Feng [a,b,c], Qiang Yu [b], Xiaoming Wang [i,*], Jianqiang He [a,b,c,**]

[a] *Key Laboratory for Agricultural Soil and Water Engineering in Arid Area of Ministry of Education, Northwest A&F University, Yangling 712100, China*
[b] *State Key Laboratory of Soil Erosion and Dryland Farming on the Loess Plateau, Institute of Water and Soil Conservation, Northwest A&F University, Yangling 712100, China*
[c] *Institute of Water-Saving Agriculture in Arid Areas of China, Northwest A&F University, Yangling 712100, China*
[d] *National Meteorological Center, Beijing 100081, China*
[e] *Sustainable Agriculture Sciences, Rothamsted Research, North Wyke, Devon EX20 2SB, UK*
[f] *Shaanxi Agricultural Remote Sensing and Economic Crop Meteorological Service Center, Xi'an 710016, China*
[g] *The UWA Institute of Agriculture and School of Agriculture and Environment, The University of Western Australia, LB 5005, Perth, WA 6001, Australia*
[h] *CIMMYT-Henan Innovation Center, Henan Agricultural University, Zhengzhou 712100, China*
[i] *State Key Laboratory of Crop Stress Biology for Arid Areas, College of Agronomy, Northwest A&F University, Yangling 712100, China*

A R T I C L E I N F O

Handling Editor: Dr. B.E. Clothier

Keywords:
CERES-Wheat
Genetic parameter
Upscaling
Regional simulating
Phenology
Spring wheat

A B S T R A C T

Cropping system models are widely used to assess the impacts of and adaptation practices to climate change on agricultural production. However, crop growth simulations at large scales have often lacked consideration of variation in crop cultivars, which were represented by different sets of genetic coefficients in crops models. In this study, taking the phenology of spring wheat (*Triticum aestivum* L.) as an example, we compared four different strategies for upscaling genetic parameters in phenology simulations at large scales with two experimental datasets. The first dataset was from field experiments comprising 40 different spring wheat cultivars at Altay (2014) and Yangling (2015–2017) station; the second dataset was historical (2010–2014) observed phenology records from 57 national agro-meteorological observation stations in China. The four strategies were the representative cultivar estimated at a single site (SSPs), the representative cultivar estimated at the 57 sites (NRPs), the various representative cultivars estimated at different agro-ecological zones (RRPs), and the virtual cultivars generated from the posterior distributions (VCPs). The posterior distributions aforesaid were established based on the calibrated parameter values of the 40 different spring wheat cultivars planted in Yangling. Then, 1000 sets of VCPs were randomly sampled from the posterior distributions. The results indicated that both the SSPs and NRPs strategy obtained large errors and uncertainties in spring wheat phenology simulations in China since only one representative cultivar was used. The RRPs strategy achieved the second high and the highest accuracy in anthesis and maturity data simulations. The VCPs strategy obtained the highest accuracy in anthesis simulation but relative larger errors in maturity simulation. The VCPs strategy can be directly used in large-scale crop growth simulations without tedious process of calibration. Hence, this strategy is recommended in areas where observations are scarce and for model users who not good at model parameter estimation.

* Corresponding author.
** Corresponding author at: Key Laboratory for Agricultural Soil and Water Engineering in Arid Area of Ministry of Education, Northwest A&F University, Yangling 712100, China.
E-mail addresses: wangxm@nwsuaf.edu.cn (X. Wang), jianqiang_he@nwsuaf.edu.cn (J. He).

https://doi.org/10.1016/j.agwat.2021.107181
Received 19 June 2021; Received in revised form 9 September 2021; Accepted 11 September 2021
Available online 21 September 2021
0378-3774/

1. Introduction

Phenology, or the timing and duration of organ formation drives plant resource acquisition (Lieth, 1974), and is a key indicator for field management practices, including fertilization (Sakamoto et al., 2010), transplantation (Brar et al., 2015), irrigation (Kar and Verma, 2005; Zhang et al., 2021). Accurate prediction of phenology is also essential for assessing the impacts of and adaptation to global climatic changes on agricultural production in large region (Angulo et al., 2013; Chen et al., 2020b; Wang et al., 2017). In recent years, cropping system models (or crop model) have been widely used to schedule field management practices or simulate crop responses to climate change (Chen et al., 2020a; He et al., 2019; Liu et al., 2020b). However, crop models were usually developed on plot or field scale and their applications were usually limited to single homogenous site (Guo et al., 2010). The concomitant heterogeneities in field environment conditions need to be considered in crop growth simulations at large scales, which was referred to "*spatializing*" the crop models (Faivre et al., 2004). However, field management information is always short, especially for the crop cultivars planted in different fields, which are described through a set of model parameters.

Key genetic parameters related to phenological variations among crop cultivars cannot be directly measured in current crop models, they were generally estimated with limited observation data using the trial-and-error method or different optimization algorithms (Wallach et al., 2019). The process parameters estimation through fitting overall field measurements is normally defined as 'model calibration'. In several recent modeling studies in large regions, crop cultivars were assumed to be uniform or directly obtained from literatures to simplify model calibration process and to save simulation time (Cammarano and Tian, 2018; Feng et al., 2019). Due to the equifinality of multiple parameter combinations, cultivar parameters estimated at single site with limited-year observations could lead to huge simulation uncertainties (He et al., 2009, 2017). At the same time, re-estimation of cultivar parameters was heavily recommended to capture spatial variations in crop growth among sub-regions (Jiang and Jin, 2009; Therond et al., 2011). Generally, cultivar parameters estimated in areas with similar conditions were effective in dealing with the scale-change errors in regional crop model simulations. However, the smaller the simulated cells were divided, the greater the data and processing time required. Thus, the question arises whether it is possible to strike a balance between easy of parameter estimation and accuracy in regional crop growth simulations?

In recent years, the Bayesian methods have seen increasing use in genetic parameter estimation in crop growth simulation models (Ceglar et al., 2011; Iizumi et al., 2009; Wallach et al., 2012). For example, He et al., (2009, 2010) compared different likelihood functions in genetic parameter estimations with the CERES-Maize model. Gao et al. (2020) compared a frequentist approach (Ordinary Least Squares, OLS) and two Bayesian approaches for the CERES-Rice model calibration and found that the Bayesian methods were promising for quantifying prediction uncertainty. In the Bayesian methods, posterior distributions of genetic parameters were generated through comparisons between model simulated and field observed variables and based on posterior distributions of genetic parameters and the Bayesian theorem. This kind of posterior distributions could be used again as posterior distributions for the re-estimation of genetic parameters of given crops when regional model simulations were conducted and the genetic characteristics of the cultivars planted were unknown (Iizumi et al., 2009). If no information was available about the crop cultivars planted in some locations, the posterior distributions derived based on experimental data from other regions might be used for parameter estimation for similar cultivars. In general, the Bayesian methods of crop parameter estimation provides an alternative method for upscaling crop cultivars in regional simulations. However, how do the cultivar parameters generated from the posterior distributions performed in phenology simulation in comparing with the simulations with different representative cultivar parameters estimated in various spatial scales.

Spring wheat is an important staple crop in China. The sown area and yield of spring wheat were about 16.1 million hectares and 6.4 million tons in 2017 (China Ministry of Agricultural, 2018). In this study, we taken spring wheat sown in China as an example and hypothesized that the simulation of spring wheat phenology with the DSSAT-CERES-Wheat model in regional scale could be improved by using virtual cultivars generated from posterior distributions of genetic parameters. The main objectives were: (1) to develop a new spatial upscaling strategy for genetic parameters related to spring wheat phenology based on Bayesian method, and (2) to compare four different spatial upscaling strategies and choose the optimal one for the simulation of spring wheat phenology in China. This work is expected to provide an alternative tool to simplify crop growth simulations at large scale with the DSSAT (Decision Support System for Agrotechnology Transfer) model by accounting for regional variation in crop cultivars.

2. Materials and methods

2.1. Model description

The DSSAT-CERES-Wheat model is a process-based model originally developed by the USDA-ARS Wheat Yield Project and the U.S. government under the AGRISTARS program (Hoogenboom et al., 2012; Jones et al., 2003; Ritchie and Otter, 1985). The DSSAT-CERES-Wheat model simulates daily wheat growth and development under varying climate, soil, and management practices. Photosynthetically active radiation and its interception by crop canopy are used to calculate potential growth, whereas actual growth on any day is limited by soil water deficits, nitrogen deficiencies, and suboptimal temperature (Ritchie, 1998). A minimum set of input data are required to run the model, including weather, crop, soil, and management practices. Soil inputs include physical, chemical, and morphological properties of each soil layer. Crop management information includes crop cultivar, planting date, depth and density, row spacing, irrigation, fertilizer, application of organic amendments, etc.

Ottman et al. (2013) reported that there were 17 related parameters affecting the phenology process in DSSAT-CERES-Wheat model, including the cultivar-type, ecotype, and species-type parameters. According to the general requirements of DSSAT model usage, the cultivar-type genetic parameters are calibrated based on observation data. The ecotype parameters could be adjusted by the experienced model users, and the species-type parameters should not be adjusted for ordinary model users. Hence, there were five parameters (Table S1) were taken into consideration in phenology simulation in this study since temperature and photoperiod are the only environmental factors affecting wheat development in the CERES-Wheat model. The ecotype parameter VEFF is the maximum allowed reduction in development rate when unvernalized. This parameter was estimated first since it affects a series of development processes and was finally set to 0.3 for this study. The cultivar parameter PHINT is the thermal time required from the end of juvenile to the end of ear growing, that was not calibrated due to the lack of required observations of leaf emergence dates. A constant value (or 95) was set for all of the related simulations in this study. Therefore, there are only three cultivar parameters (P1V, P1D, and P5) were estimated for each specific cultivar in this study. The genetic parameters were estimated with the DSSAT-GLUE package, which is based on the generalized likelihood uncertainty estimation (GLUE) method (Mertens et al., 2004; He et al., 2009 and 2010).

2.2. Study areas and datasets

Spring wheat was grown from northeast to southwest China (green shaded areas in Fig. 1) with obvious different climate conditions. Most spring wheat was sown in areas with cold and dry climate in northern China. In these areas, mean annual cumulative thermal time (≥10 °C)

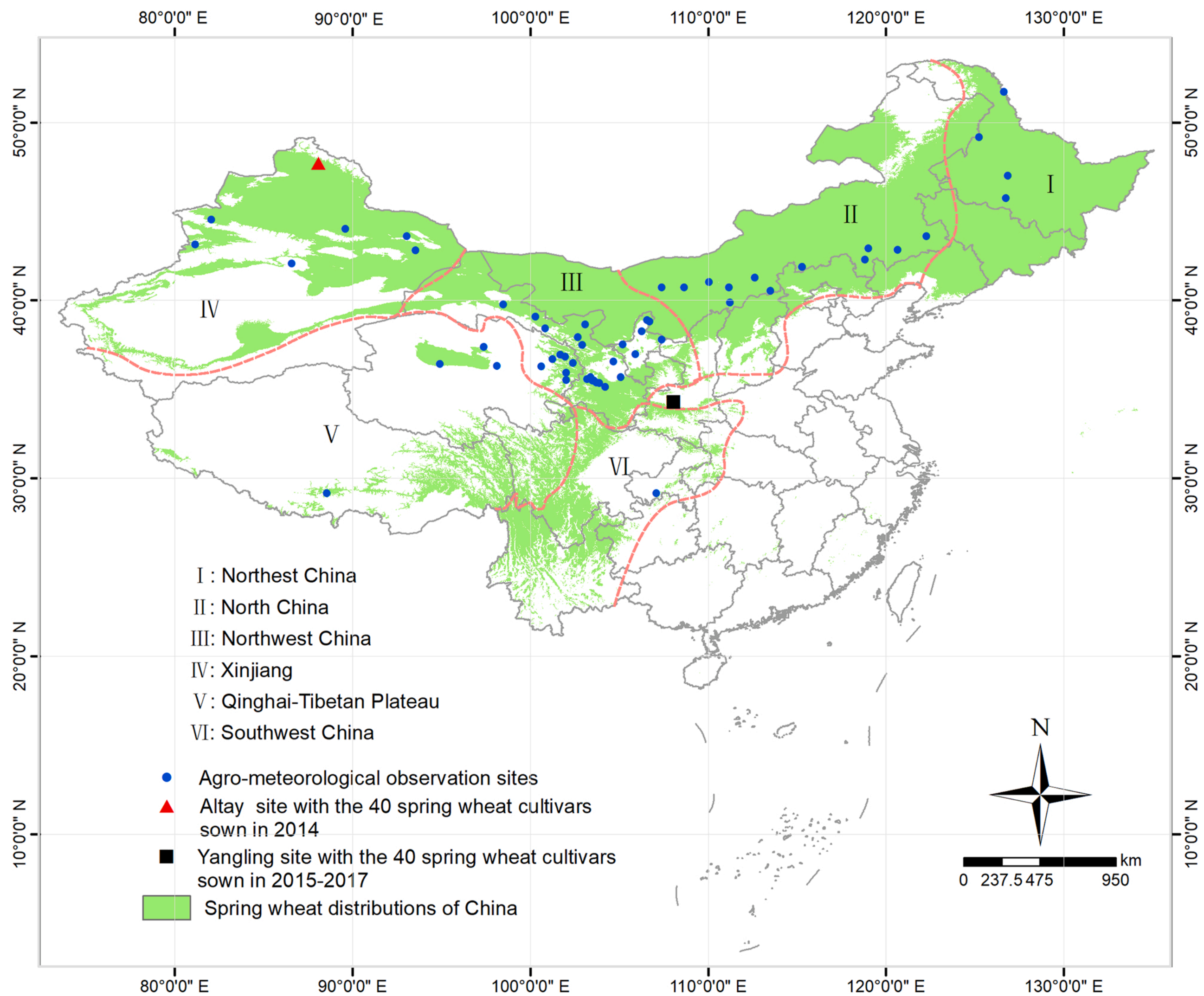

Fig. 1. Distribution of the agro-ecological zones of spring wheat (green shaded areas), the experiment sites sown with the 40 spring wheat cultivars (Yangling in Shaanxi Province, black square; Altay in Xinjiang Province, red triangle), and the 57 agro-meteorological observation sites (blue dots) of the Chinese Meteorology Administration (CMA). The 57 stations represented six different agro-ecological zones (AEZ) in China, namely the northeast China (Zone I), north China (Zone II), northwest China (Zone III), Xinjiang (Zone Ⅳ), the Qinghai-Tibetan Plateau (Zone V), and southwest China (Zone Ⅵ) (Zhao, 2010). And the same below. (For interpretation of the references to colour in this figure legend, the reader is referred to the web version of this article.)

was about 2750 °C·d with variations from 1650° to 3620°C·d. The mean temperatures of the coldest month (January) and day were −10 °C and −30 °C, respectively. The extreme low temperatures prevent wheat from overwintering, thus only spring wheat could be sown. Expect for the spring wheat regions, there were also some areas where both spring and winter wheat were sown. These regions were mainly located in the plateau areas in western China, including the Qinghai-Tibetan Plateau, the Yunnan-Guizhou Plateau. In these areas, the mean annual cumulative thermal time (≥10 °C) was about 2050 °C·d with variations from 84° to 4610 °C·d. The mean temperatures of the coldest month (January) were close to −10 °C. It was noteworthy that winter temperature was mild enough in the Yunnan-Guizhou Plateau in southwest China. In these areas, spring wheat is sown in the fall (Oct-Dec), which was also named 'fall-sown spring wheat' and is grown mainly in rotation with rice. Both spring-sown and fall-sown spring wheat were taken into consideration since the observations under these two grown schedules were both collected and used in this study.

Two datasets of spring wheat phenology were used for different purposes in this study. The first dataset was from field experiments of multiple spring wheat cultivars conducted at Altay (47°43′N, 88°05′E, 735 m) in Xinjiang Province in 2014, and at Yangling (34°17′N, 108°04′E, 506 m) in Shaanxi Province in 2015–2017 (Table 1). For the experiment conducted at Altay, the 40-cultivar experiment was sown on April 16th in 2014. For the experiment conducted at Yangling, spring wheat was sown at four different sowing dates in both 2015–2016 and 2016–2017 growing seasons (Table S2), which resulted in a range of different photoperiods and accumulative temperatures. Sufficient irrigation water and fertilizer were applied at the two sites to avoid water and nutrient stresses during the growing seasons. All treatments were managed to avoid water or nutrient stress and effects of weeds and pests. There were three replicates for each treatment. This dataset was mainly used to establish the posterior distributions of genetic parameters related to spring wheat phenology in the DSSAT-CERES-Wheat model.

The second dataset comprised phenology observations of rainfed spring wheat at 57 agro-meteorological experimental stations, which belonged to the Chinese Meteorology Administration (CMA), in China from 2010 to 2014 (Table S3; Fig. 1). We divided these 57 sites into six agro-ecological zones (AEZs): northeast China (Zone I), north China (Zone II), northwest China (Zone III), the Qinghai-Tibetan Plateau (Zone Ⅳ), Xinjiang (Zone V), and southwest China (Zone Ⅵ) (Zhao, 2010; Liu et al., 2020a). It is noteworthy that in the vast subtropical and tropical climate areas (Zone Ⅵ), including the Sichuan Basin and the

Table 1
Summary of the field experiment of 40 spring wheat cultivars and four different sowing dates at Yangling in northwest China.

Site	Growing season	Sowing date	Mean anthesis (DAS)[a]	Mean maturity (DAS)	RGP length (d)[b]	Average temperature (°C)[c]	Accumulated rainfall (mm)
Yangling	2015–2016	2015/10/08	198 (1.6[d])	239 (0.7)	41	9.1	204
		2015/11/20	162 (1.1)	203 (4.0)	41	9.0	123
		2015/12/30	127 (1.6)	170 (1.2)	43	11.0	117
		2016/ 02/18	79 (1.1)	115 (3.8)	36	14.9	110
	2016–2017	2016/10/18	186 (1.2)	225 (0.7)	39	9.2	246
		2016/11/18	170 (1.3)	200 (3.3)	30	9.3	289
		2016/12/28	138 (2.1)	166 (0.9)	28	11.1	311
		2017/02/19	98 (1.0)	125 (1.1)	27	15.8	301
Altay	2014	2014/4/16	63 (2.9)	108 (3.2)	45	17.7	37

[a] DAS = days after sowing;
[b] RGP = reproductive growing period;
[c] Average temperature of the growing season;
[d] Standard deviations of phenology date observations of the 40 different cultivars.

Yunnan-Guizhou Plateau, spring wheat was usually sown in fall (October or November) (Yu et al., 1995). Information about crop management was obtained from on-farm observations. Management practices at each site, including fertilizer application and weed control, were generally the same as or better than the conventional practices by local farmers. Plant protection management was undertaken to guarantee optimum growth and avoid weeds and pests. Observations included days from sowing to anthesis and maturity, which were conducted by trained agricultural technicians according to standardized observation methods (CMA, 1993). All phenology data were obtained from the National Meteorological Information Center (NMIC) of the Chinese Meteorology Administration. This dataset comprehensively represents the production status of spring wheat in China since geographic locations of these sites roughly covered all of the spring wheat regions in China. This dataset was mainly used for evaluating the four different upscaling strategies of cultivar parameters for phenology simulated with DSSAT-CERES-Wheat.

Soil water parameters, including saturated soil moisture, residual soil moisture and soil hydraulic conductivity, were obtained from the China Soil Hydraulic Parameters Dataset (Dai et al., 2013). Daily weather data included daily maximum and minimum air temperature, daily rainfall, and daily global solar radiation. For all sites, weather data were obtained from the China Meteorological Data Sharing Service System (http://cdc.cma.gov.cn/). Solar radiation data were not available, so daily cumulative solar radiation was estimated based on daylength and sunshine hours with the Angstrom-Prescott formula (Angstrom, 1924; Prescott et al., 1940).

2.3. Upscaling strategies for cultivar parameters in regional simulation of spring wheat growth

Four upscaling strategies for cultivar genetic parameter estimations of spring wheat were established and evaluated in this study based on the two experimental datasets (Fig. 2). These four strategies could be divided into two kinds of solutions. The first kind directly estimated the genetic parameters of representative cultivar at different geographic scales, which was established based on the 5-year field records of anthesis and maturity dates at the 57 agro-meteorological obsevation stations in China. The second sloution tried to summarize the distributions of genetic parameters for the spring wheat cultivars sown in China. This solution was established based on the field observations of the experiments conducted at Altay in 2014 and Yangling in 2015–2017 with 40 widely-sown spring wheat cultivars. The four upscaling strategies were compared in simulations of anthesis date, maturity date, and grain-filling duration at all of the 57 gero-meteorological stations.

2.3.1. Strategy 1: Single site parameters (SSPs)

In many studies, cultivars planted in a given region were assumed to be the same to simplify modeling and reduce simulation time. Cultivar genetic parameters, which were estimated only based on the observations of a single site, were then used in crop growth simulations in large regions. Following this strategy, we assumed that the different spring wheat cultivars were sown at the 57 agro-meteorological observation station. To explore the simulation uncertainties caused by various cultivars at large scale, each of the 57 different cultivars was parameterized at its individual station and then validated at the other 56 stations. All the 5-year observed anthesis and maturity dates were used to estimate the cultivar genetic parameters for each site with the DSSAT-GLUE package. In this study, we mainly focused on the variability of the SSPs in phenology simulations. Since 57 different SSPs were generated, we did not compare this strategy with the rest upscaling strategies at site scale.

2.3.2. Strategy 2: National representative parameters (NRPs)

Due to the equifinality of multiple parameter combinations, cultivar parameters estimated at a single site under limited years could lead to large uncertainties (He et al., 2009, 2017). In this strategy, the observed anthesis and maturity dates from all of the 57 sites in 2010 were used for the estimation of genetic parameters of a national representative cultivar, or NRPs. Then, this set of national representative parameters or NRPs were validated based on the data of 2011–2014 for all of the 57 sites.

2.3.3. Strategy 3: Regional representative parameters (RRPs)

In this strategy, we assumed that an individual representative cultivar was sown in each agro-ecological zone (AEZ) of spring wheat production in China. In each AEZ, the observed anthesis and maturity dates from all local sites in 2010 were used to estimate the genetic parameters of the regional representative cultivar, or RRPs. Then, the RRPs were validated with the rest observations in 2011–2014 in each AEZ.

2.3.4. Strategy 4: Virtual cultivar parameters (VCPs) generated from the posterior parameter distributions

For the 40 cultivars sown at Altay and Yangling, the genetic parameters of each cultivar were estimated based on the observations of four sowing-date treatments in the experiment conducted at Yangling in the 2015–2016 growing season. Next, the estimated genetic parameters were further validated at Altay in 2014 and Yangling in 2016–2017 growing seasons. Third, the distributions of the estimated values of the three genetic parameters (P1V, P1D, and P5) were tested using the '*fitdistrplus*' package of R (Delignette-Muller and Dutang, 2015); R Core Team, 2020). The judgement of potential distribution of the target dataset by the '*fitdistrplus*' package relies on the specific relationship between skewness and kurtosis. Then, 1000 sets of genetic parameters were randomly sampled following the established posterior distributions with R. All these 1000 virtual spring wheat cultivars were then used to simulate the spring wheat experiment conducted in Altay (red triangle in Fig. 1) to validate the posterior distributions and the sampling method. Finally, the 1000 virtual cultivars were used to simulate the

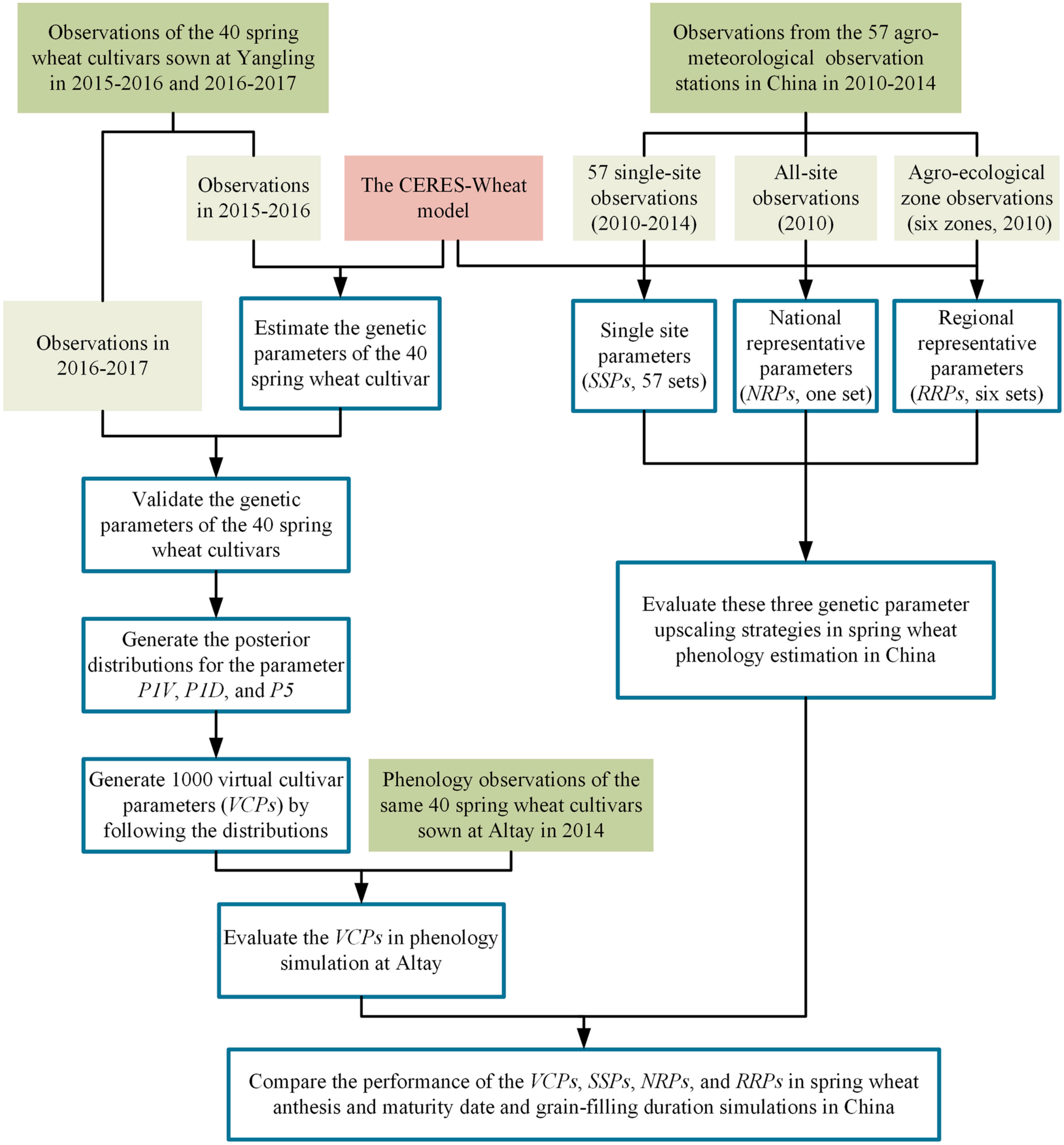

Fig. 2. Flowchart of the four upscaling strategies of cultivar genetic parameter of spring wheat in phenology simulation with the DSSAT-CERES-Wheat model in China.

anthesis and maturity dates of spring wheat at all the 57 agro-meteorological observation stations in 2010–2014. To compare with the other three upscaling strategies, the average value of the 1000 model runs with the 1000 virtual cultivars were treated as the final simulation result for each site.

2.4. Statistics for model performance evaluation

Since a total of 40 different spring wheat cultivars were grown at Yangling at each sowing date were repeated three times, the standard deviation (SD, Eq. 1) were used to evaluate the variations in anthesis and maturity dates of these cultivar.

$$SD = \sqrt{\frac{1}{n}\sum_{i=1}^{n}\left(O_i - \overline{O}\right)^2} \tag{1}$$

where O_i and $\overline{O}$ were the observed and their mean value of given variables, n was the repeated times.

Many different indices have been proposed to evaluate the discrepancies between simulations and measurements (Wallach et al., 2019). In this study, we concentrated on three measures to show the different aspects of regional simulation accuracy with the four upscaling strategies for cultivar genetic parameters of spring wheat. The root mean square error (RMSE, Eq. 2) has the advantage to express errors in the same unit as the variable.

$$RMSE = \sqrt{\frac{1}{n}\sum_{i=1}^{n}(S_i - O_i)^2} \quad (2)$$

where S_i and O_i were simulated and observed values of given variables, respectively; and n was the number of simulation times.

To compare the variables likely to give a broad range of crop response, the relative error could provide another sight from the absolute error. For example, anthesis dates of spring wheat mainly ranged from 50 to 100 days after sowing (das), while maturity dates were nearly 1.5 times of it. Thus, we also calculated the relative root mean square error (RRMSE, Eq. 3) and coefficient of determination (R^2, Eq. 4) to evaluate the simulation accuracy of anthesis and maturity with different upscaling strategies.

$$RRMSE = \frac{RMSE}{\overline{O}} \times 100\% \quad (3)$$

$$R^2 = \frac{\left[\sum_{i=1}^{n}\left(O_i - \overline{O}\right)\left(S_i - \overline{S}\right)\right]^2}{\sum_{i=1}^{n}\left(O_i - \overline{O}\right)^2 \sum_{i=1}^{n}\left(S_i - \overline{S}\right)^2} \quad (4)$$

3. Results

3.1. Uncertainties in phenology simulation using the SSPs

Small RMSEs were achieved for the both phenology stages during calibration, with an average value of 3.7 d and 3.9 d (from 0.9 to 8.5) for anthesis and maturity dates (Fig. 3), respectively. As expected, RMSE values increased during validation, with an average value of 6.4 (5.4–10.7) d and 10.8 (8.5–18.4) d for anthesis and maturity, respectively. The results indicated that large errors and uncertainties were caused when using the site-specific cultivar simulate in phenology simulations in large area, especially in maturity date (Fig. 3b). The lowest errors were obtained with the parameters calibrated in Zone 1 (northeast China) for anthesis and maturity in both calibration and validation processes. In addition, there were no obvious differences in the simulation accuracies with the genetic parameters calibrated in different AEZs.

3.2. Calibration and validation of the NRPs and RRPs

The NRPs (National representative parameters) and RRPs (Regional representative parameters) were calibrated and validated based on the observations from the 57 stations in 2010 and 2011–2014 (Fig. 4), respectively. There were six sets of RRPs since this up-scaling strategy were conducted in each of the six different AEZ. Generally, the simulation errors of anthesis were smaller than maturity during both calibration and validation processes. The RMSE values were ranged from 5.7 to 6.9 d and from 8.3 to 10.3 d for the two phenology stages, respectively. Additionally, the estimation errors of the NRPs were greater than the RRPs for both anthesis and maturity date simulations both in calibration and calibration. Compared with the NRPs, the RMSE values of the RRPs reduced by 0.8 d and 0.4 d for calibrations and validations of anthesis, but 2.0 d and 0.7 d for calibrations and validations of maturity. The results indicated that the RRPs improved regional maturity simulations. In addition, it was noteworthy that the CERES-Wheat model was able to simulate phenology of the autumn-sown spring wheat (the five points in the top-right corner of each sub-figure, Fig. 4). Small simulation errors were obtained in most years of this experiment even with the NRPs (Fig. 4a), which employed only one cultivar to represent spring wheat in the whole China.

3.3. Generation and evaluation of the VCPs

3.3.1. Calibration and validation of the genetic parameters of the 40 cultivars

The genetic parameters of the 40 spring wheat cultivars were calibrated based on the field observation in 2015–2016 growing season at Yangling, and validated at Altay in 2014 and Yangling in the 2016–2017 growing seasons (Fig. 5). Great variations were obtained for the durations from sowing to anthesis and to maturity, which were resulted from the four sowing dates. The anthesis dates were 76–201 DAS and 97–189 DAS in the 2015–2016 and 2016–2017 growing season, and the maturity dates were 111–241 DAS and 124–228 DAS, respectively. Overall, the 40 sets of estimated cultivar genetic parameters simulated anthesis and maturity well for all of the four sowing-date treatments since all data points were close to the 1:1 line. The results showed that the 40 sets calibrated cultivar genetic parameters could reproduce the annual difference among different sowing dates. The RMSE values were 6.5 d and 5.2 d for anthesis and maturity simulations in the calibration process, respectively. Then, the 40 calibrated cultivar genetic parameters were validated at both Yangling and Altay, where the climate conditions and

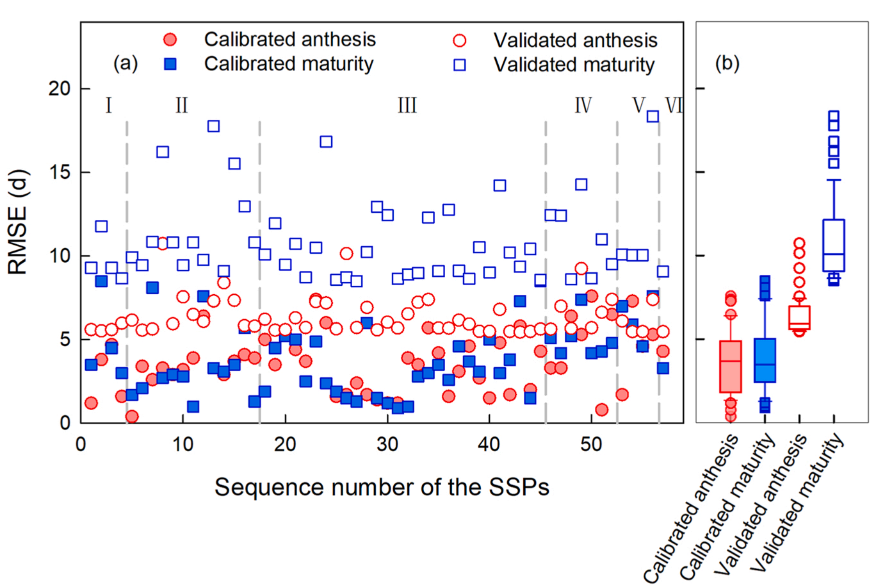

Fig. 3. Calibration and validation of the 57 site-specific genetic parameters (or SSPs) estimated for each of the 57 stations (a) and the general uncertainty (b). The red filled, red empty, blue filled, and blue empty symbols represent the RMSE values of anthesis date in calibration, anthesis date in validation, maturity date in calibration, and maturity date in validation, respectively. (For interpretation of the references to colour in this figure legend, the reader is referred to the web version of this article.)

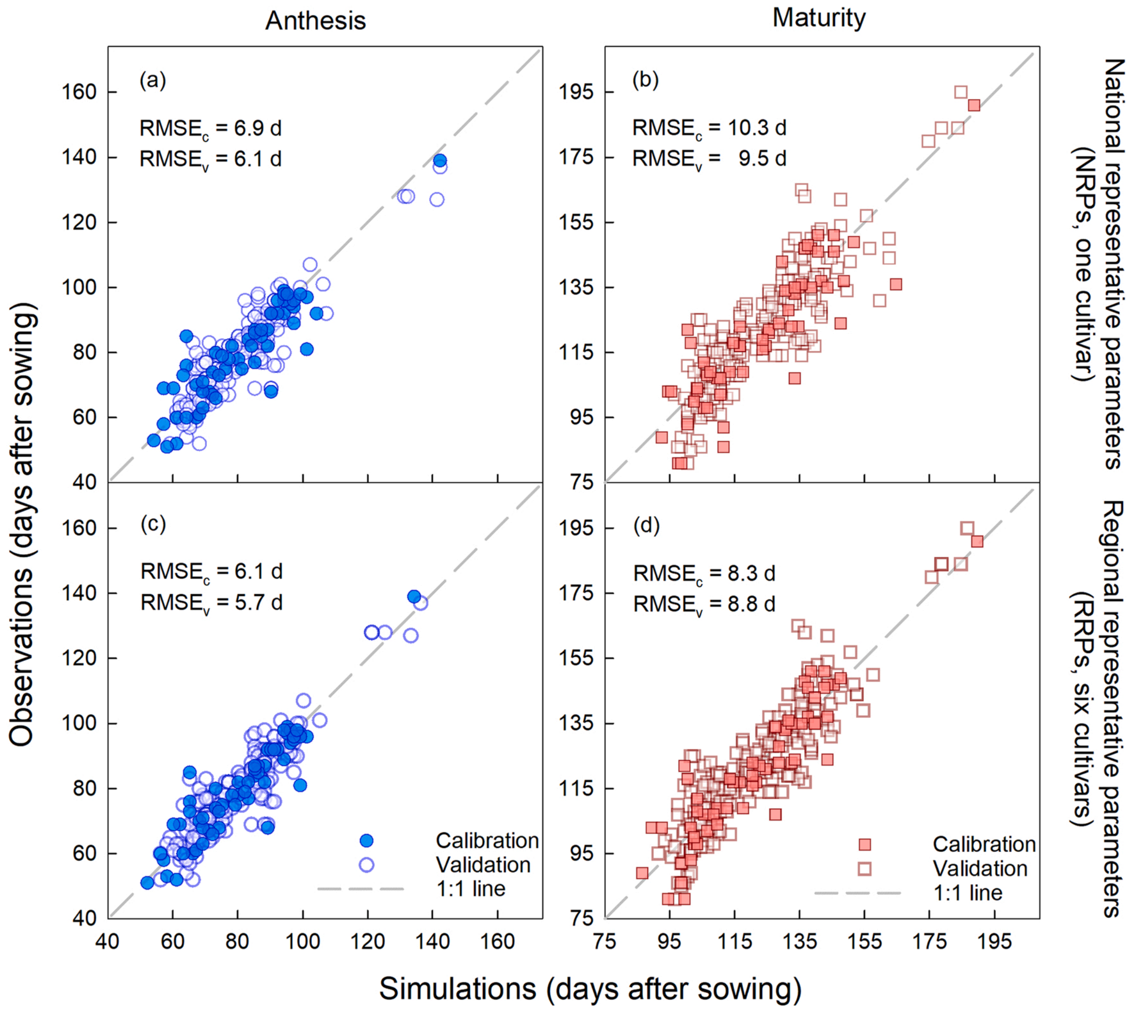

Fig. 4. Model calibration and validation based on the upscaling strategies of the national representative parameters (NRPs; a, b) and the regional representative parameters (RRPs; c, d) in China. In each upscaling strategy, the observed anthesis and maturity dates in 2010 (filled symbols) were used for model calibration, and the observations in 2011–2014 (empty symbols) were used for model validation. The grey dashed line is the 1:1 line. RMSE$_c$ and RMSE$_v$ indicate root mean square error (RMSE) between simulations and observations in model calibration and validation, respectively.

farming schedules were greatly different from Yangling. However, greater simulation errors were generated during calibrations. Compared with the results of validation at Yangling, the RMSE values were increased by 3.6 d and 1.3 d for the two phenology stages in calibrations using observations from 2015 to 2016. Smaller simulations were obtained for both the two sites during validation. The RMSE values were 2.9 d and 3.2 d for anthesis at Yangling and Altay, and were 3.9 d and 4.2 d for maturity, respectively.

3.3.2. *Generation of the posterior parameter distributions and VCPs*

The statistical distributions of P1V, P1D, and P5 of the 40 spring wheat cultivars were explored based on the '*fitdistrplus*' package of R (Figs. S1 and S2). The results indicated that P1V and P5 approximately followed the uniform and logistical distributions, respectively. However, no common distribution was found for P1D. Overall, it was difficult to determine the real distributions of these parameters based on the limited number of estimated parameter values. We then tried another three possible distributions for the parameter P1D, including normal, lognormal, and logistical distribution, and also applied the logistic distribution for the parameter P5 (Table S4). Apart from the original uniform distributions for the three cultivar parameters, three kinds of distributions of P1D were combined with the uniform distribution of P1V (Fig S1b) and logistic distribution of P5 (Fig S1c), respectively. In each combination, 1000 sets of virtual cultivar parameters (VCPs) were generated. The 1000 sets of VCPs separately generated from each kind of P1D distribution were used to simulate spring wheat phenology at Altay in 2014 (Fig. S3). Compared to the original uniform-distribution assumption, same median values of anthesis and maturity dates were provided by the logistic, normal, and lognormal distributions of P1D. Additionally, the mean values of the two phenology stages were also similar to each other. Hence, the assumption of uniform distributions for the three cultivar parameters were acceptable since the mean prediction values of multiple VCPs were used to represent the daily phenology prediction within growing seasons. Considering the difficulty in parameter sampling, the uniform distribution assumption was accepted in this study. Finally, for simplicity we assumed that all these three parameters followed uniform distributions (represented by maximum and minimum values). Finally, the new posterior distributions of phenology related genetic parameters were established for further regional simulations (Eq. 5).

$$\text{Parameter distributions} = \begin{cases} P1V \sim U(8.7, 16.0) \\ P1D \sim U(50.2, 65.7) \\ P5 \sim U(559.7, 657.1) \end{cases} \tag{5}$$

Following the above posterior parameter distributions of genetic parameters, 1000 sets of VCPs were sampled and used to simulate the anthesis and maturity dates of the 40 spring wheat cultivars sown at Altay in 2014 (Fig. 6). Compared with the observations, simulations

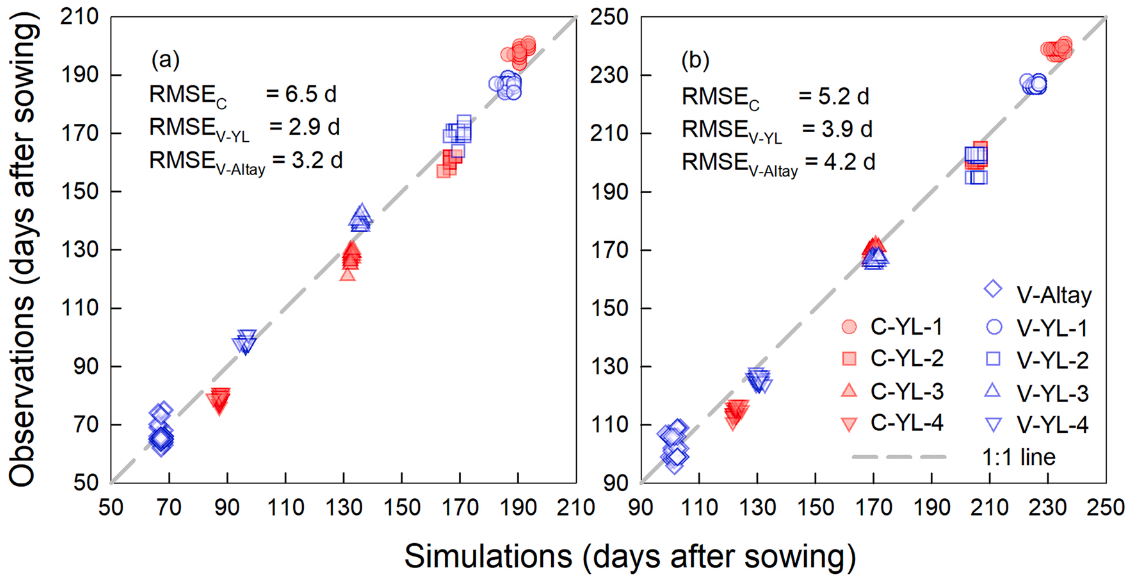

Fig. 5. Calibration and validation of anthesis (a) and maturity (b) dates of the 40 spring wheat cultivars sown in the field experiments conducted at Altay in 2014 and Yangling in 2015–2017 growing seasons. The observations from Yangling in the 2015–2016 growing season (red filled symbols) were used for the calibration of genetic parameters of the 40 cultivars, while validations were conducted at both Yangling (blue empty symbols with the same shapes) and Altay (blue empty diamonds). Circles, squares, upper triangles, and lower triangles indicate the first, second, third, and fourth sowing date in the two growing seasons at Yangling, respectively. The grey dashed line is the 1:1 line. The symbol *C*, *V* and *YL* represents calibration, validation and Yangling, respectively. RMSE$_c$ and RMSE$_v$ indicate the root mean square error (RMSE) in model calibration and validation. (For interpretation of the references to colour in this figure legend, the reader is referred to the web version of this article.)

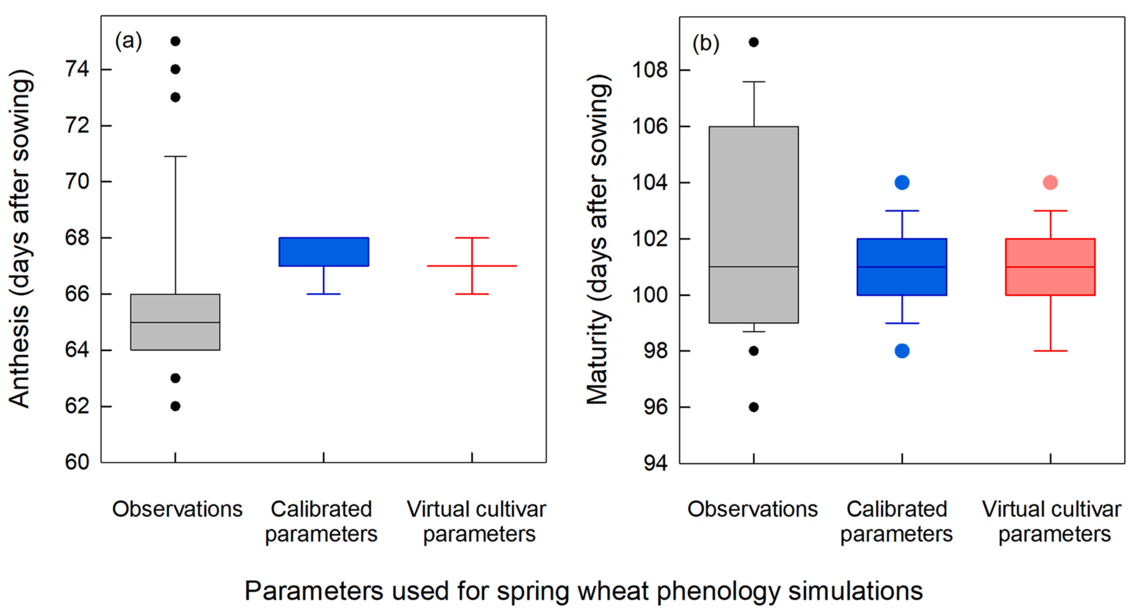

Fig. 6. Comparisons between the observed and simulated anthesis (a) and maturity (b) dates for the 40 spring wheat cultivars sown at Altay in 2014. The blue and red boxes represent the simulations with the 40 sets of estimated genetic parameters and 1000 VCPs, respectively. (For interpretation of the references to colour in this figure legend, the reader is referred to the web version of this article.)

with the 40 calibrated cultivar parameters and with 1000 VCPs had less variations for both anthesis and maturity dates. The VCPs almost obtained same anthesis and maturity simulations as the 40 calibrated cultivars since same ranges (anthesis: 66–68 d; maturity: 98–104 d) and median values (anthesis: 67 d; maturity: 101 d) were obtained for both the two phenology stages. The results showed that the VCPs, which were sampled assuming a uniform distribution, could well represent the parameter distributions for phenology of spring wheat. Besides, ranges of the simulated anthesis and maturity dates were covered by the corresponding field observations, which showed less variation of the VCPs in phenology simulation. However, the median values of the simulations were close to the observations since the difference between the median values of simulations and observations were 2 d for anthesis and 0 d for maturity.

3.4. Comparisons among phenology simulations using NRPs, RRPs, and VCPs

The annual and five-year RMSE and RRMSE values were calculated for the estimations of anthesis and maturity dates of the 57 stations using the NRPs, RRPs, and VCPs (Fig. 7). The simulated anthesis dates were better than the simulated maturity dates since values ranged 4.7–7.0 d and 8.3–11.4 d for anthesis and maturity simulations, respectively. However, the difference between the simulation accuracies of the two phenology stages were smaller in the term of RRMSE ranged 5.9–9.4% and 6.5–9.6% for anthesis and maturity dates, respectively. Besides, there were obvious differences among phenology stage simulations with different up-scaling strategies. Simulations with NRPs had the lowest accuracy for anthesis and maturity since this strategy only used one set of genetic parameters to represent the spring wheat sown in China. The five-year average RMSE values were 6.3 d and 9.6 d, and RRMSE values were 8.0% and 7.9% for anthesis and maturity. The RRPs achieved the second highest and the highest accuracy for anthesis and maturity simulations, respectively. Compared with the NRPs, the average simulation RMSE errors were reduced by 0.5 d for anthesis and 1.0 d for maturity; and RRMSE values were reduced by 0.7% for anthesis and 0.8% for maturity, respectively. However, the VCPs achieved the smallest simulation errors in anthesis date simulations but the largest errors in maturity date simulations. The average RMSE values were 5.2 d and 9.6 d and RRMSE values were 6.6% and 7.9% for anthesis and maturity, respectively.

The average RMSE values of the 57 sites were 5.0 d, 4.7d and 4.4 d for the NRPs, RRPs and VCPs, respectively. The three upscaling strategies had similar performance in reducing the simulation errors (Fig. 8). The number of stations with RMSE value less than 3 d were 17, 18, and 18 for the NRPs, RRPs and VCPs. However, the VCPs performed better in the upper limit of simulation errors since no site had RMSE value greater than 12 d, while there were three stations for both the NRPs and RRPs. The maximum values of RMSE were 19.4, 18.0 and 10.6 d for the NRPs, RRPs and VCPs, respectively. The results also indicated that the largest variation occurred in regional anthesis date simulations with only one national representative cultivar. Generally, the RMSE values were less than 6 d for the most stations, and the numbers of such stations were 44, 47 and 47 for the NRPs, RRPs and VCPs. The worst regional simulation accuracies were obtained in Zone Ⅵ for both the NRPs (RMSE = 7.1 d) and VCPs (RMSE = 9.6 d), where spring wheat was sown in autumn due to the high temperature. However, these two upscaling strategies both used the same cultivar sets (one set in the NRPs and 1000 sets in the VCPs) in spring wheat anthesis simulation in large area without local calibration, which might explain the poor performance in this region. Compared with the NRPs and VCPs, the RRPs obtained smaller RMSE value (4.9 d) in Zone Ⅵ. The lowest regional simulation accuracy of the RRPs was obtained in Zone II with RMSE value = 5.8 d, which was much smaller than the NRPs and VCPs. The best performance in phenology simulations in AEZ level with the RRPs were caused by the same scale of parameter calibration for this upscaling strategy.

Compared with anthesis, the simulations of maturity had larger RMSE values for all 57 stations (Fig. 8b, d and f). Only seven (or 12% of total) sites investigated had a RMSE value less than 3 d with the NRPs, while the numbers were both eight with the RRPs and VCPs. On the contrary, the number of sites with RMSE values greater than 12 d were eight with the NRPs, seven with the RRPs and 12 with the VCPs. The average RMSE values of the 57 sites were 8.1 d, 7.3 d and 8.0 d for the NRPs, RRPs and VCPs, respectively. The VCPs generated the largest maturity estimation errors since the RMSE values ranged from 1.2 to 27.2 d. The RMSE values ranged 1.6–26.4 d and 0.8–21.2 d for the NRPs and RRPs (Fig. S4), respectively. However, the 95th-percentiles value of RMSE of VCPs was smaller than those provided by the NRPs. Finally, the smallest simulation errors were all obtained in Zone Ⅵ, with the RMSE values were 6.4, 5.4 and 3.8 d for the NRPs, RRPs and VCPs. The lowest accuracies were in Zone Ⅴ for both the NRPs (RMSE = 13.8 d) and VCPs (RMSE = 15.7 d), and in Zone I for the RRPs (RMSE = 7.9 d).

For the VCPs strategy, the 12 stations with RMSE value greater than 12 d were mainly located at the high-altitude places, where the average elevation was 2080 m and the average annual air temperature was 6.6 ℃ (Table 3). The large errors in maturity simulations with the VCPs (RMSE = 7.5 d) were probably caused by the poor performance in grain-

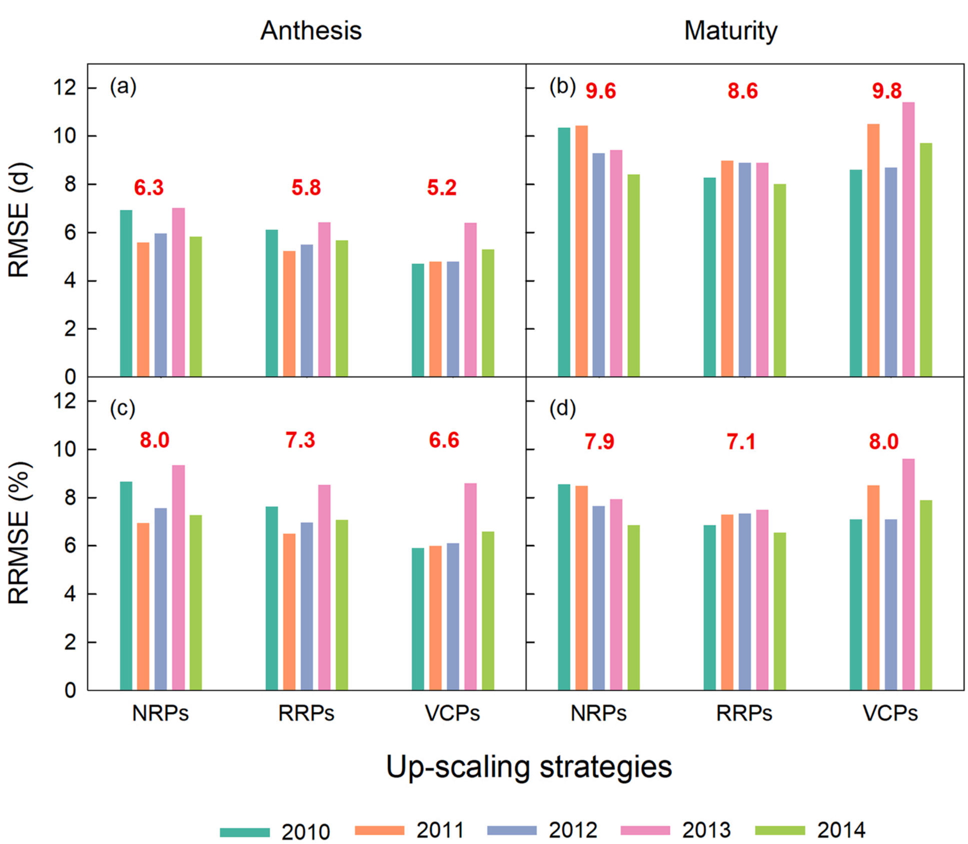

Fig. 7. Annual variations of the root mean square error (RMSE) and the relative root mean square error (RRMSE) for the anthesis (a, c) and maturity (b, d) date simulations with three upscaling strategies of genetic parameters at the 57 agro-meteorological observation sites in China in 2010–2014. The symbols NRPs, RRPs and VCPs represent the upscaling strategy of national representative parameters, regional representative parameters, and virtual cultivar parameters, respectively. The five-year average values (red) of each statistic were provided above the corresponding bars. (For interpretation of the references to colour in this figure legend, the reader is referred to the web version of this article.)

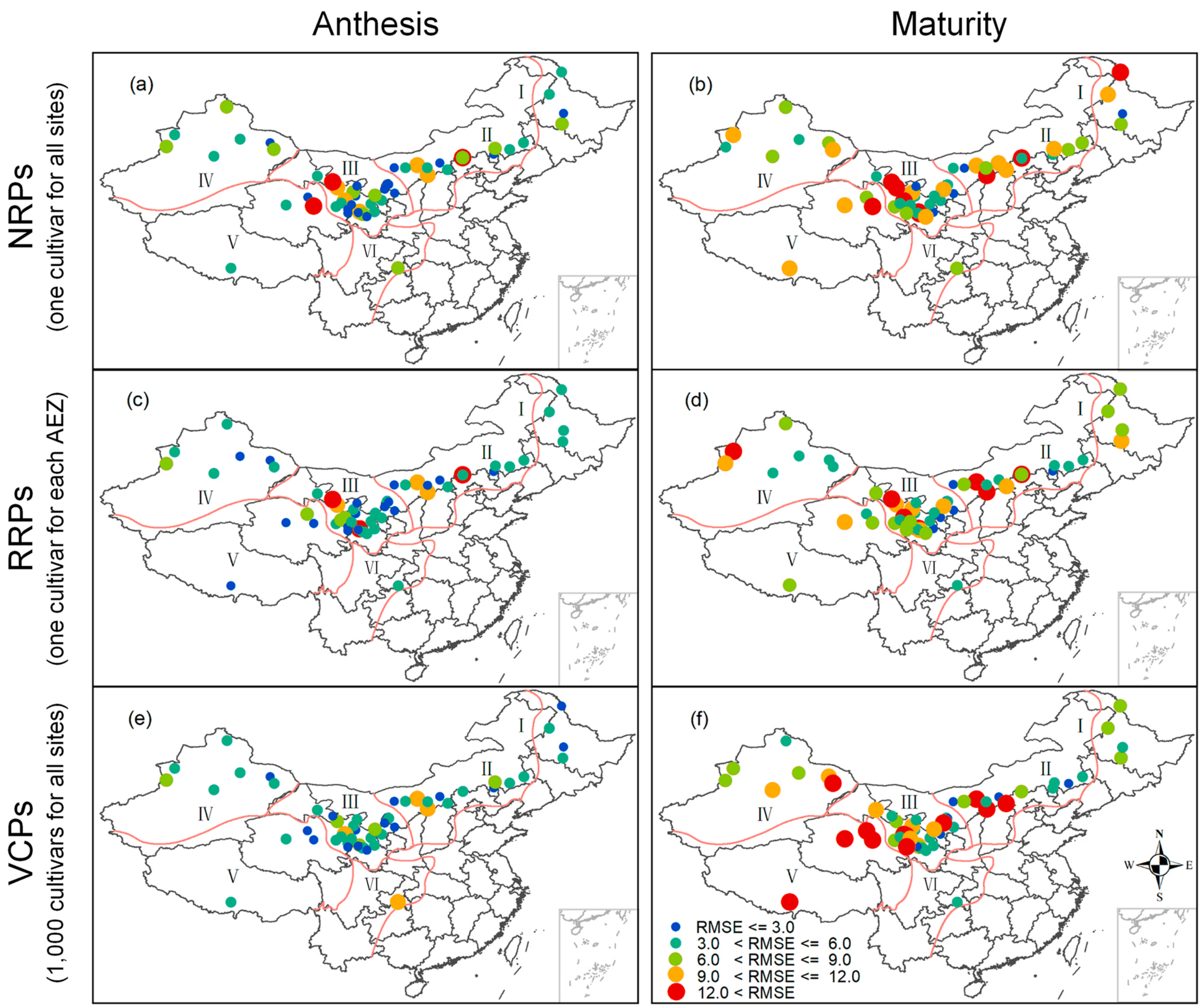

Fig. 8. Spatial distributions of the root mean square errors (RMSEs) between the observed and estimated anthesis (a, c, e) and maturity (b, d, f) dates with three upscaling strategies of cultivar genetic parameters at the 57 agro-meteorological observation sites of China in 2010–2014. The three strategies were the national representative parameters (or NRPs, a and b), regional representative parameters (or RRPs, c and d), and virtual cultivar parameters (or VCPs, e and f), respectively. The blue, cyan, green, orange and red circles indicate the sites with values of RMSE < 3 d, 3–6 d, 6–9 d, 9–12 d, and > 12 d, respectively. The numbers of cultivars used in phenology simulation were one for NRPs, six for RRPs, and 1000 for VCPs. (For interpretation of the references to colour in this figure legend, the reader is referred to the web version of this article.)

filling duration simulations (Fig. 9, S5). Compared with the VCPs, the data points provided by the NRPs and RRPs were closer to the 1:1 line. The RMSE values of the NRPs, RRPs, and VCPs were 7.1, 6.9, and 8.7 d, respectively. There were obvious underestimations of the grain-filling duration with the VCPs, especially in areas with longer grain-filling requirement (observed grain-filling duration > 55 d). Besides, the R^2 values of the VCPs was the highest among the three upscaling strategies.

4. Discussion

4.1. Phenology simulations with single representative cultivar (SSPs and NRPs)

The single representative cultivar assumption has been widely used in crop growth simulations at large scales (Chen et al., 2018; Sun et al., 2018; Xiao and Tao, 2014). In this study, all of the 57 SSPs provided low simulation errors for both anthesis and maturity dates at their relevant sites. Liu et al. (2020a) also reported that high accuracy was obtained at site scale with detailed inputs related to crop growth. However, large errors were generated by most individual SSPs when using them in simulations at other stations. This is mainly because parameters are often highly related to their testing conditions and are less universal (He et al., 2009). Additionally, He et al. (2017) reported the equifinality of different combinations of cultivar parameters calibrated at a single site (He et al., 2017). Hence, large uncertainty would be generated in regional crop growth simulations with single-site calibrated cultivar parameters.

The results of the SSPs indicated the importance of using observations from different climate conditions in parameter calibration and model validation. Therefore, we developed the NRPs strategy by using all of the 57-station observations in 2010 to parameterize the cultivar. Compared with the SSPs, the simulation errors were reduced. Besides, good simulation accuracy was also achieved at the Nanchuan station (the five points in the top-right corners of Fig. 4a and b), where spring wheat was sown in autumn. However, the one representative cultivar assumption was contradicted the actual production situation, especially in a country with a wide range of climates such as China. In addition, massive data of different climatic zones were required in the estimation of cultivar genetic parameters in this strategy. However, field observations were usually scarce in many countries, which would result in

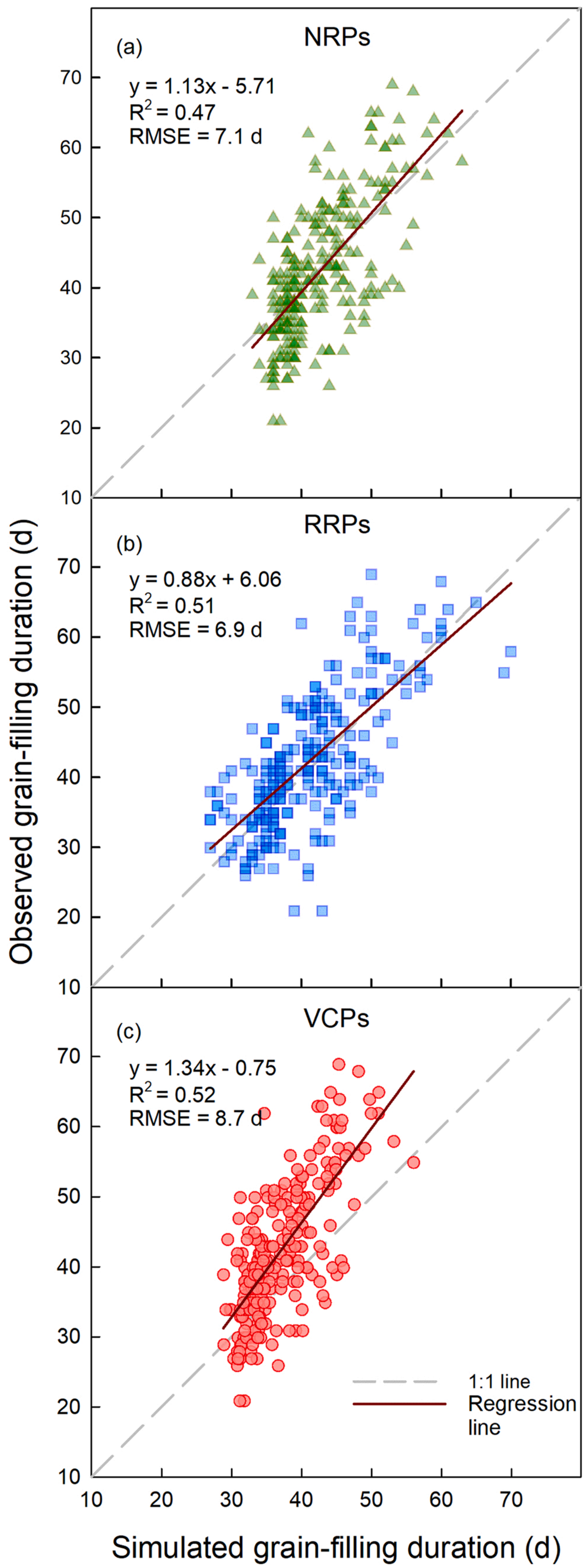

(caption on next column)

Fig. 9. Observed and estimated grain-filling durations of spring wheat simulated with the genetic parameters generated with three upscaling strategies at the 57 agro-meteorological observation stations of China in 2010–2014. The three strategies were the national representative parameters (NRPs; green triangle), regional representative parameters (RRPs; blue square), and virtual cultivar parameters (VCPs; red circle), respectively. The grey dashed line is the 1:1 line. (For interpretation of the references to colour in this figure legend, the reader is referred to the web version of this article.)

invalid simulations in the large scales (Xiong et al., 2014).

4.2. Phenology simulations with multiple representative cultivars (RRPs and VCPs)

Compared with the SSPs and NRPs, the highest and second highest simulation accuracies were provided by this strategy for maturity and anthesis, respectively. The representative cultivar parameters estimated in large scales showed great potential in regional crop growth simulations. Jiang and Jin (2009) also reported that the genetic parameters estimated in the AEZ level provided the highest simulations accuracy for rice in Jiangsu Province in China. Therond et al. (2011) estimated the genetic parameters of maize and wheat in regional scale and applied these parameters in the simulations across 12 European countries. Compared with the simulations with only one representative cultivar, the accuracies were substantially improved with the regional representative cultivar. However, the RRPs strategy increased the difficulty and time consumption in the estimations of cultivar genetic parameter. Besides, this strategy was also invalid when observation data were scarce.

In this study, several possible distributions (uniform, normal, lognormal, and logistic) were assumed for the three cultivars parameters. Then, different VCPs were sampled from different combinations of these distributions and validated at Altay. The results indicated that similar anthesis and maturity dates were simulated with different parameter distributions. Hence, we defined P1V, P1D and P5 followed the uniform distributions. Gao et al. (2020) and Ma et al. (2020) also accepted the uniform-distribution assumption for the three parameters. The results demonstrated the uniform distribution was reasonable since the similar ranges and median values of anthesis and maturity date simulations were obtained by the randomly sampled VCPs and the 40 sets of calibrated parameters. However, variations of anthesis and maturity date simulations with the VCPs and the calibrated parameters were both smaller than the observations at Altay. It was mainly because the parameterization of the 40 cultivars were conducted based on the experiments at Yangling, where phenology observations taken small variations. The VCPs obtained the smallest simulation errors for anthesis date, which indicated good estimations for the parameter P1V and P1D. Hunt et al. (1993) pointed that the parameter P5 was the most sensitive parameter affecting grain-filling duration. Hence, the VCPs obtained second highest simulation errors in maturity date due to underestimation of the grain-filling duration, which indicated the parameterization deviation of the parameter P5. For the 12 stations with RMSE > 12 d with the VCPs strategy (Table 2), the frigid climate conditions might let local farmers sow spring wheat cultivars different from the 40 cultivars involved in our study. Xiong (2009) evaluate the CERES-Wheat model in wheat growth simulations in China. They pointed that the largest simulation errors were obtained in the 8th and 9th AZE with high altitudes, which was similar as the region III and V in this study, with RMSE values greater than 35%. In general, more experimental observations of more spring wheat cultivars sown in various areas were needed to modify the posterior distribution for parameter P5.

4.3. Comparisons among the four upscaling strategies

In this study, four upscaling strategies for cultivar genetic parameters of spring wheat were established and evaluated. In general, the simulation errors of maturity date were greater that anthesis date for all of

Table 2
Location and climatic information of the 12 national agro-meteorological observation sites with the root mean square error (RMSE) values greater than 12 d in maturity date simulation with the virtual cultivar parameters (VCPs).

Site name	AEZ	Site index	Elevation (m)	Longitude (°)	Latitude (°)	Annual mean temperature (°C)	Annual mean rainfall (mm)	RMSE (d)
Guyang	II	8	1360	110.05	41.03	5.5	386.8	16.2
Xinghe	II	7	1269	113.5	40.52	5.5	425.7	15.4
Kailu	II	13	241	111.22	39.87	7.2	385.2	12.2
Datong	III	43	2450	102.02	35.93	5.5	639.7	27.2
Huzhu	III	40	2480	100.62	36.27	4.9	587.3	17.6
Yongning	III	21	1114	106.25	38.25	10.9	232.2	14.7
Tongren	III	42	2491	101.68	36.95	7	524.5	12.9
Hami	IV	47	737	93.52	42.82	10.5	48.8	13.4
Shigatse	V	53	3836	102.4	36.48	7.4	518.1	18.1
Golmud	V	55	2808	102.83	36.33	6.5	59.2	17.1
Delhi	V	54	2982	94.9	36.42	4.8	289	14.3
Dulan	V	56	3189	126.63	51.73	3.6	294.2	13.1

the four strategies. Three sources of uncertainties were involved in the agricultural and environmental modeling, namely equations, input variables, and parameter values (Wallach et al., 2019). Models are simplifications of the real world to some extent by using huge amount of equations. However, errors were introduced when using these equations to reproduce crop growth processes. For example, the simulation of maturity date was based on the simulation of anthesis and grain-filling duration. More processes with corresponding errors were involved in the simulation of maturity date than in the simulation of anthesis date. Wallach et al. (2017) reported that the model structure generated larger uncertainty than model parameters. The poor performance of the CERES-Wheat model in maturity date simulations might be caused by the unclear mechanism. Nouna et al. (2003) and Yao et al. (2020) reported that the CERES series models provided large simulation errors under serious water stress. The spring wheat was all rainfed at the 57 stations, which might suffer from water stress since rainfall were mainly occurred in summer in our study area. The second possible reason for the greater errors in maturity data simulation might be the erroneous maturity observation. Seidel et al. (2019) reported that the availability of spatial and temporal data has become the main limitation for crop modeling (Seidel et al., 2019). The input data that well represent the production situation of the target area were essential for reliable simulations (Xiong et al., 2019). The third possible reason was the insufficient parameterization of the parameters that affect the phenology processes. As reported by Ottman et al. (2013), 17 parameters affect wheat phenology processes in the DSSAT-CERES-Wheat model. However, we only estimated four of them and mainly focused on the three cultivar genetic parameters (P1V, P1D, and P5). Higher prediction accuracy might be achieved by taking into consideration of more parameters. In addition, Messina et al. (2006) suggested that the estimations of cultivar genetic parameters should take into account the genetic information. A gene-based system for estimating genetic specific parameters might offer better long-term prospects for reducing simulation error, making it easier to apply models at regional to global scales (White et al., 2008).

Generally, there were several advantages for the VCPs strategy in crop growth simulations at regional scales. First, variations in spring wheat cultivars were involved in regional simulations, which was impossible by the SSPs and NRPs strategy. Next, the uncertainties generated by crop cultivars were taken into account in regional simulations, which were usually ignored in many previous studies of crop growth response to climate changes in large area. Third, this strategy accounted for the variations of crop cultivars since 1000 sets of virtual cultivars were used in simulations, which might contain the cultivar that was exactly sown in the study area. Fourth, this strategy was possible to help explain the interactions of genotype (G) × environment (E) × management (M). Finally, this strategy was ideal for places where basic experimental observations were extremely scarce. The virtual cultivars generated with the posterior parameter distributions could be used directly in areas lacking of field measurements.

However, the disadvantages of the VCPs strategy were also apparent. First, crop growth simulations and analysis became further complicated by considering the crop cultivar uncertainties. Next, model runs and time consumption are dramatically increased. If the 1000 virtual cultivars generated from the posterior parameter distributions were all applied in growth simulations, the number of model runs would be 1000 times of that using only one representative cultivar. With the increases available of high-performance computing platforms, the time-consuming problem of large number of model runs could be expected to be solved. Finally, different sampling sizes will be tried to evaluate the performance of the VCPs in regional simulations, through which the minimum optimal number of virtual cultivar parameters might be found.

5. Conclusions

Few simulation studies have examined the uncertainties caused by cultivar differences in large-scale simulations despite the wide use of crop models. Among the four upscaling strategies, the SSPs and NRPs strategies generated considerable errors in anthesis and maturity dates throughout China. Therefore, we do not recommend these strategies in regions with obviously different field management practices. The RRPs strategy provided more reliable simulation accuracy comparing with the SSPs and NRPs, but the data requirement was massive and the parameter calibration processes were complex and time consuming. Therefore, this strategy is not recommended where observation data are scarce. According to the VCPs strategy, using an ensemble of different spring wheat cultivars (summarized as genetic parameter distributions) could account for the unknown sown cultivars in large-scale crop growth simulations. Besides, the virtual spring wheat cultivars could be directly sampled from the simple uniform distributions without local calibration. It was reasonable to expect that the consideration of uncertainty in crop cultivars will contribute to more reliable simulations of crop growth at large scales. Generally, we recommended both RRPs and VCPs strategies in regional spring wheat phenology simulations and the RRPs strategy was more suitable for maturity date estimations in large regions containing a wide range of climates.

Declaration of Competing Interest

The authors declare that they have no known competing financial interests or personal relationships that could have appeared to influence the work reported in this paper.

Acknowledgments

This research was partially supported by the Natural Science Foundation of China (No. 52079115, 41961124006), the Key Research and Development Program of Shaanxi (N0. 2019ZDLNY07-03), the Key Research and Development Program of Shaanxi (No. 2020ZDLSF06-02), the "111 Project" (No. B12007) of China, and the NERC Newton Fund (NE/S009094/1) of UK. We are also grateful to the three anonymous reviewers whose comments and suggestions have greatly improved this manuscript.

Appendix A. Supporting information

Supplementary data associated with this article can be found in the online version at doi:10.1016/j.agwat.2021.107181.

References

Angstrom, A., 1924. Solar and terrestrial radiation. Report to the international commission for solar research on actinometric nvestigations of solar and atmospheric radiation. Q. J. Roy. Meteor. Soc. 50 (210), 121–126.

Angulo, C., Rötter, R., Lock, R., Enders, A., Fronzek, S., Ewert, F., 2013. Implication of crop model calibration strategies for assessing regional impacts of climate change in Europe. Agric. Meteorol. 170, 32–46.

Brar, A.S., Buttar, G.S., Jhanji, D., Sharma, N., Vashist, K.K., Mahal, S.S., Deol, J.S., Singh, G., 2015. Water productivity, energy and economic analysis of transplanting methods with different irrigation regimes in Basmati rice (Oryza sativa L.) under north-western India. Agric. Water Manag. 158, 189–195.

Cammarano, D., Tian, D., 2018. The effects of projected climate and climate extremes on a winter and summer crop in the southeast USA. Agric. Meteorol. 248, 109–118.

Ceglar, A., Črepinšek, Z., Kajfež-Bogataj, L., Pogačar, T., 2011. The simulation of phenological development in dynamic crop model: the Bayesian comparison of different methods. Agric. . Meteorol. 151 (1), 101–115.

Chen, S., Jiang, T., Ma, H., He, C., Xu, F., Malone, R.W., Feng, H., Yu, Q., Siddique, K.H. M., Dong, Qg, He, J., 2020a. Dynamic within-season irrigation scheduling for maize production in Northwest China: a method based on weather data fusion and yield prediction by DSSAT. Agric. For. Meteorol. 285–286, 107928.

Chen, Y., Donohue, R., McVicar, T., Waldner, F., Mata, G., Ota, N., Houshmandfar, A., Dayal, K., Lawes, R., 2020b. Nationwide crop yield estimation based on photosynthesis and meteorological stress indices. Agric. For. Meteorol. 284, 107872.

Chen, Y., Zhang, Z., Tao, F., 2018. Impacts of climate change and climate extremes on major crops productivity in China at a global warming of 1.5 and 2.0°C. Earth Syst. Dyn. 9, 543–562.

China Ministry of Agricultural, 2018. Chinese Agricultural Statistics 2017. China Agricultural Press, Beijing (in Chinese).

Dai, Y., Shangguan, W., Duan, Q., Liu, B., Fi, S., 2013. Development of a China dataset of soil hydraulic parameters using pedotransfer functions for land surface modeling. J. Hydrometeorol. 14 (3), 869–887.

Delignette-Muller Laure, Marie, Dutang, Christophe, 2015. fitdistrplus: An R Package for Distribution Fitting Methods. Journal of Statistical Software 64 (4). https://doi.org/10.18637/jss.v064.i04.

Faivre, R., Leenhardt, D., Voltz, M., Benoît, M., Papy, F., Dedieu, G., Wallach, D., 2004. Spatialising crop models. Agronomie 24 (4), 205–217.

Feng, P., Wang, B., Liu, D.L., Waters, C., Yu, Q., 2019. Incorporating machine learning with biophysical model can improve the evaluation of climate extremes impacts on wheat yield in south-eastern Australia. Agric. Meteorol. 275, 100–113.

Gao, Y., Wallach, D., Liu, B., Dingkuhn, M., Boote, K.J., Singh, U., Asseng, S., Kahveci, T., He, J., Zhang, R., Confalonieri, R., Hoogenboom, G., 2020. Comparison of three calibration methods for modeling rice phenology. Agric. For. Meteorol. 280, 107785.

Guo, R., Lin, Z., Mo, X., Yang, C., 2010. Responses of crop yield and water use efficiency to climate change in the North China Plain. Agric. Water Manag. 97 (8), 1185–1194.

He, D., Wang, E., Wang, J., Lilley, J.M., 2017. Genotype × environment × management interactions of canola across China: A simulation study. Agric. Meteorol. 247, 424–433.

He, J., Dukes, M.D., Jones, J.W., Graham, W.D., Judge, J., 2009. Applying GLUE for estimating CERES-maize genetic and soil parameters for sweet corn production. Trans. ASABE 52 (6), 1907–1921.

He, J., Jones, J.W., Graham, W.D., Dukes, M.D., 2010. Influence of likelihood function choice for estimating crop model parameters using the generalized likelihood uncertainty estimation method. Agric. Syst. 103 (5), 257–264.

He, L., Jin, N., Yu, Q., 2020. Impacts of climate change and crop management practices on soybean phenology changes in China. Sci. Total Environ. 707, 135638.

Hoogenboom, G., J.W. Jones, P.W. Wilkens, C.H. Porter, K.J. Boote, L.A. Hunt, U. Singh, J.L. Lizaso, J.W. White, O. Uryasev, F.S. Royce, R. Ogoshi, A.J. Gijsman, G.Y. Tsuji, and J. Koo. 2012. Decision Support System for Agrotechnology Transfer (DSSAT) Version 4.5 [CD-ROM]. University of Hawaii, Honolulu, Hawaii.

Hunt, L.A., Pararajasingham, S., Jones, J.W., Hoogenboom, G., Imamura, D.T., Ogoshi, R. M., 1993. GENCALC: software to facilitate the use of crop models for analyzing field experiments. Agron. J. 85, 1090–1094.

Iizumi, T., Yokozawa, M., Nishimori, M., 2009. Parameter estimation and uncertainty analysis of a large-scale crop model for paddy rice: spplication of a Bayesian approach. Agric. Meteorol. 149 (2), 333–348.

Jiang, M., Jin, Z., 2009. A method for upscaling genetic parameters of CERES-Rice in regional. Rice Sci. 16 (4), 292–300.

Jones, J.W., Hoogenboom, G., Porter, C.H., Boote, K.J., Batchelor, W.D., Hunt, L.A., Wilkens, P.W., Singh, U., Gijsman, A.J., Ritchie, J.T., 2003. The DSSAT cropping system model. Eur. J. Agron. 18 (3), 235–265.

Kar, G., Verma, H.N., 2005. Phenology based irrigation scheduling and determination of crop coefficient of winter maize in rice fallow of eastern India. Agric. Water Manag. 75 (3), 169–183.

Lieth, H., 1974. Phenology and Seasonality Modeling. Springer-Verlag, New York.

Liu, H., Pequeno, D.N.L., Hernández-Ochoa, I.M., Krupnik, T.J., Sonder, K., Xiong, W., Xu, Y., 2020a. A consistent calibration across three wheat models to simulate wheat yield and phenology in China. Ecol. Model. 430, 109132.

Liu, Y., Tang, L., Qiu, X., Liu, B., Chang, X., Liu, L., Zhang, X., Cao, W., Zhu, Y., 2020b. Impacts of 1.5 and 2.0°C global warming on rice production across China. Agric. For. Meteorol. 284, 107900.

Ma, H., Malone, R.W., Jiang, T., Yao, N., Chen, S., Song, L., Feng, H., Yu, Q., He, J., 2020. Estimating crop genetic parameters for DSSAT with modified PEST software. Eur. J. Agron. 115, 126017.

Mertens, J., Madsen, H., Feyen, L., Jacques, D., Feyen, J., 2004. Including prior information in the estimation of effective soil parameters in unsaturated zone modelling. J. Hydrol. 294 (4), 251–269.

Messina, C.D., Jones, J.W., Boote, K.J., Vallejos, C.E., 2006. A gene-based model to simulate soybean developmentand yield responses to environment. Crop Sci. 46, 456–466.

Nouna, B.B., Katerji, N., Mastrorilli, M., 2003. Using the CERES-maize model in a semi-arid Mediterranean environment. New modelling of leaf area and water stress functions. Eur. J. Agron. 19 (2), 115–123.

Ottman, M.J., Anthony Hunt, L., White, J.W., 2013. Photoperiod and vernalization effect on anthesis date in winter-sown spring wheat regions. Agron. J. 105 (4), 1017–1025.

Prescott, J.A., Prescott, J., Prescott, J.S., 1940. Evaporation from a water surface in relation to solar radiation. Trans. Roy. Soc. S. Aust. 64, 114–118.

R Core Team, 2020. R: A language and environment for statistical computing. R foundation for Statistical Coumpting, Vienna. ⟨https://www.r-project.org/⟩.

Ritchie, J.T., Otter, S., 1985. Description and performance of CERES-Wheat: A User-Oriented Wheat Yield Model ARS-U. S. Dep. Agric. Res. Serv. Mo.

Ritchie, J.T., 1998. Soil water balance and plant water stress. In: Tsuji, G.Y., Hoogenboom, G., Thornton, P.K. (Eds.), Understanding Options for Agricultural Production. Kluwer Academic, Dordrecht, The Netherlands, pp. 41–54.

Sakamoto, T., Wardlow, B.D., Gitelson, A.A., Verma, S.B., Suyker, A.E., Arkebauer, T.J., 2010. A two-step filtering approach for detecting maize and soybean phenology with time-series MODIS data. Remote Sens. Environ. 114 (10), 2146–2159.

Seidel, S.J., Barfus, K., Gaiser, T., Nguyen, T.H., Lazarovitch, N., 2019. The influence of climate variability, soil and sowing date on simulation-based crop coefficient curves and irrigation water demand. Agric. Water Manage. 221, 73–83.

Sun, S., Yang, X., Lin, X., Sassenrath, G.F., Li, K., 2018. Climate-smart management can further improve winter wheat yield in China. Agric. Syst. 162, 10–18.

Therond, O., Hengsdijk, H., Casellas, E., Wallach, D., Adam, M., Belhouchette, H., Oomen, R., Russell, G., Ewert, F., Bergez, J.-E., Janssen, S., Wery, J., Van Ittersum, M.K., 2011. Using a cropping system model at regional scale: low-data approaches for crop management information and model calibration. Agric. Ecosyst. Environ. 142 (1–2), 85–94.

Wallach, D., Keussayan, N., Brun, F., Lacroix, B., Bergez, J.-E., 2012. Assessing the uncertainty when using a model to compare irrigation strategies. Agron. J. 104 (5), 1274–1283.

Wallach, D., Makowski, D., Jones, J.W., Brun, F., 2019. Working with dynamic crop models. Methods, Tools, and Exemples for Agriculture and Evcironment, third ed. Academic Press.

Wallach, D., Nissanka, S.P., Karunaratne, A.S., Weerakoon, W.M.W., Thorburn, P.J., Boote, K.J., Jones, J.W., 2017. Accounting for both parameter and model structure uncertainty in crop model predictions of phenology: a case study on rice. Eur. J. Agron. 88, 53–62.

Wang, E., Martre, P., Zhao, Z., Ewert, F., Maiorano, A., Rotter, R.P., Kimball, B.A., Ottman, M.J., Wall, G.W., White, J.W., Reynolds, M.P., Alderman, P.D., Aggarwal, P. K., Anothai, J., Basso, B., Biernath, C., Cammarano, D., Challinor, A.J., De Sanctis, G., Doltra, J., Dumont, B., Fereres, E., Garcia-Vila, M., Gayler, S., Hoogenboom, G., Hunt, L.A., Izaurralde, R.C., Jabloun, M., Jones, C.D., Kersebaum, K.C., Koehler, A.K., Liu, L., Muller, C., Naresh Kumar, S., Nendel, C., O'Leary, G., Olesen, J.E., Palosuo, T., Priesack, E., Eyshi Rezaei, E., Ripoche, D., Ruane, A.C., Semenov, M.A., Shcherbak, I., Stockle, C., Stratonovitch, P., Streck, T., Supit, I., Tao, F., Thorburn, P., Waha, K., Wallach, D., Wang, Z., Wolf, J., Zhu, Y., Asseng, S., 2017. The uncertainty of crop yield projections is reduced by improved temperature response functions. Nat. Plants 3, 17102.

White, J.W., Herndl, M., Hunt, L.A., Payne, T.S., Hoogenboom, G., 2008. Simulation-based analysis of effects of Ppd and Vrn loci on flowering in wheat. Crop Sci. 48, 678–687.

Xiao, D., Tao, F., 2014. Contributions of cultivars, management and climate change to winter wheat yield in the North China Plain in the past three decades. Eur. J. Agron. 52, 112–122.

Xiong, W., 2009. The performance of CERES-Wheat model in wheat planting areas and its uncertainties. J. Appl. Meteor. Sci. 20 (1), 88–94 (In Chinese with English abstract).

Xiong, W., Asseng, S., Hoogenboom, G., Hernandez-Ochoa, I., Robertson, R., Sonder, K., Pequeno, D., Reynolds, M., Gerard, B., 2019. Different uncertainty distribution between high and low latitudes in modelling warming impacts on wheat. Nat. Food 1 (1), 63–69.

Xiong, W., Balkovič, J., van der Velde, M., Zhang, X., Izaurralde, R.C., Skalský, R., Lin, E., Mueller, N., Obersteiner, M., 2014. A calibration procedure to improve global rice yield simulations with EPIC. Ecol. Model. 273, 128–139.

Yao, N., Li, Y., Xu, F., Liu, J., Chen, S., Ma, H., Chau, H.W., Liu, D.L., Li, M., Feng, H., Yu, Q., He, J., 2020. Permanent wilting point plays an important role in simulating

winter wheat growth under water deficit conditions. Agric. Water Manag. 229, 105954.
Yu, S., Nan, C., Tian, L., 1995. Common wheat ecological divisions and classification in China I Common wheat ecoogical divisions in China. Acta Agric. Boreal. -Sin. 10 (4), 6–13 (In Chinese with English abstract).
Zhang, H., Ma, L., Douglas-Mankin, K.R., Han, M., Trout, T.J., 2021. Modeling maize production under growth stage-based deficit irrigation management with RZWQM2. Agric. Water Manag. 248.
Zhao, G., 2010. Study on Chinese wheat planting regionalization (II). J. Triticeae Crop. 30 (6), 1140–1147 (In Chinese with English abstract).